

RESEARCH ARTICLE

Pharmacological and genetic inhibition of downstream targets of p38 MAPK in experimental nephrotic syndrome

Xiaojing Nie,^{1,2} Melinda A. Chanley,¹ Ruma Pengal,¹ David B. Thomas,³ Shipra Agrawal,^{1,4*} and William E. Smoyer^{1,4*}

¹Center for Clinical and Translational Research, The Research Institute at Nationwide Children's Hospital, Columbus, Ohio;

²Department of Pediatrics, Fuzhou Dongfang Hospital, Xiamen University, Fuzhou, China; ³University of Miami Miller School of Medicine, Miami, Florida; and ⁴Department of Pediatrics, College of Medicine, The Ohio State University, Columbus, Ohio

Submitted 19 April 2017; accepted in final form 21 November 2017

Nie X, Chanley MA, Pengal R, Thomas DB, Agrawal S, Smoyer WE. Pharmacological and genetic inhibition of downstream targets of p38 MAPK in experimental nephrotic syndrome. *Am J Physiol Renal Physiol* 314: F602–F613, 2018. First published November 29, 2017; doi:10.1152/ajprenal.00207.2017.—The p38 MAPK pathway plays a crucial role in various glomerulopathies, with activation being associated with disease and inhibition being associated with disease amelioration. We hypothesized that the downstream targets of p38 MAPK, MAPK-activated protein kinase 2 and/or 3 (MK2 and/or MK3), play an important role in mediating injury in experimental nephrotic syndrome via their actions on their downstream substrates heat shock protein B1 (HSPB1) and cyclooxygenase-2 (COX-2). To test this hypothesis, the effects of both pharmacological and genetic inhibition of MK2 and MK3 were examined in mouse adriamycin (ADR) and rat puromycin aminonucleoside (PAN) nephropathy models. MK2^{-/-}, MK3^{-/-}, and MK2^{-/-}MK3^{-/-} mice were generated in the Sv129 background and subjected to ADR-induced nephropathy. MK2 and MK3 protein expression was completely abrogated in the respective knockout genotypes, and massive proteinuria and renal histopathological changes developed after ADR treatment. Furthermore, renal cortical HSPB1 was induced in all four genotypes by *day 21*, but HSPB1 was activated only in the wild-type and MK3^{-/-} mice. Expression of the stress proteins HSPB8 and glucose-regulated protein 78 (GRP78) remained unaltered across all genotypes. Finally, while MK2 and/or MK3-knockout downregulated the proinflammatory enzyme COX-2, ADR significantly induced renal cortical COX-2 only in MK2^{-/-} mice. Additionally, pharmacological MK2 inhibition with PF-318 during PAN-induced nephropathy did not result in significant proteinuria reduction in rats. Together, these data suggest that while the inhibition of MK2 and/or MK3 regulates the renal stress response, our currently available approaches are not yet able to safely and effectively reduce proteinuria in experimental nephrotic syndrome and that other p38MAPK downstream targets should also be considered to improve the future treatment of glomerular disease.

glomerular disease; inhibition; MAPK; MK2; MK3; nephrotic syndrome; p38; proteinuria

INTRODUCTION

Currently available therapies for nephrotic syndrome (NS), including glucocorticoids, have many side effects and are frequently ineffective in focal segmental glomerulosclerosis (FSGS) which is one of the most important causes of acquired chronic kidney disease (CKD) (24, 25). The p38 MAPK signaling pathway is known from both animal and human studies to play a crucial role in glomerular disease, where activation has been associated with disease activation and inhibition has been associated with disease amelioration (16, 30, 51, 56). Indeed, it has been reported that p38 MAPK may be a desirable potential target for therapeutic intervention in NS, including FSGS (30). However, since p38 MAPK signaling plays an important role in diverse cellular processes, attempts to utilize p38 MAPK inhibitors in clinical trials for many other types of diseases have been unsatisfactory due to their significant side effects (15, 18). Interestingly, downstream of p38 MAPK are two additional kinases, MAPK-activated protein kinases 2 and 3 (MK2 and MK3), which are phylogenetically related protein kinases that serve as direct substrates of p38 MAPK (41, 48). In exploration of the potential utility of inhibition of such downstream kinases as therapeutic targets, we have previously reported the specific role of this downstream signaling pathway, p38 MAPK→MK2/MK3→heat shock protein B1 (HSPB1), in both in vitro models of podocyte injury and in an in vivo model of acute glomerulonephritis (20, 38). Additionally, we have also identified cyclooxygenase-2 (COX-2) as an additional p38 MAPK-dependent mediator of podocyte pathophysiology (3, 38). Based on the above, we hypothesized that the downstream targets of p38 MAPK, MK2 and/or MK3, play an important role in mediating injury in experimental NS via its actions on its downstream substrates HSPB1 and COX-2. To test this hypothesis, we examined the effects of both pharmacological and genetic inhibition of MK2 and MK3 in puromycin aminonucleoside (PAN)-induced and in adriamycin (ADR)-induced nephropathy in rats and mice, respectively. We generated mice and studied the development of NS in the presence or absence of MK2 and/or MK3 genetic deletions in an ADR-susceptible strain (sv129) and analyzed the roles of each kinase in regulating proteinuria, renal morphology, renal cortical activation, and the expression of specific small heat shock proteins (sHSPs) and the proinflammatory enzyme COX-2. Additionally, we studied the safety and

* S. Agrawal and W. E. Smoyer are co-senior authors and contributed equally to this work.

Address for reprint requests and other correspondence: S. Agrawal, Center for Clinical and Translational Research The Research Institute at Nationwide Children's Hospital, 700 Children's Dr., Columbus, OH 43205 (e-mail: shipra.agrawal@nationwidechildrens.org).

efficacy of pharmacologic inhibition of MK2 (PF-318) (4, 14) in experimental NS in rats.

MATERIALS AND METHODS

Breeding, generation, and genotyping of MK2/MK3 knockout mice.

This study was performed in accordance with the animal protocols approved by the Institutional Animal Care and Use Committee. MK2/MK3 double heterozygous mice (MK2^{+/-} MK3^{+/-}) in C57BL/6 background were backcrossed with WT 129/SvJ female mice (Jackson Laboratory, Bar Harbor, ME) for seven generations to obtain MK2, MK3, and MK2/MK3 knockout (KO) mice in an ADR-susceptible strain. Mice were genotyped by PCR analysis of alkaline-lysed toe clips as previously described (32, 41). WT alleles were discriminated from KO alleles using an amplicon that spans the 5' LoxP insertion site of either MK2 or MK3 gene. The MK2-WT allele was detected using the forward (5'-CATGCCATGATGAGGTGCCTCTGC) and reverse primers (5'-CCCTCTCTACCTCTTTCTGTGAATGCC) resulting in an amplicon of 200 bp. The MK2-KO allele was detected by using the same forward primer (5'-CATGCCATGATGAGGTGCCTCTGC) and reverse primer specific for neomycin resistance cassette (5'-CCCTCTCTACCTCTTTCTGTGAATGCC) resulting in an amplicon of 560 bp. The MK3-WT allele was detected using the forward (5'-GCCAATGTCGCCGATTATCTCTGC) and reverse primers (5'-CAGGGAGCACTCACAGAGCAGTGGGC) resulting in an amplicon of 879 bp. MK3-KO allele was detected by using the same forward primer (5'-GCCAATGTCGCCGATTATCTCTGC) and reverse primer specific for neomycin resistance cassette (5'-CTGTTGTGCCAGTCATAGCCG) resulting in an amplicon of 1,239 bp. The PCR products were separated on 1.5% agarose gels and visualized by ethidium bromide staining. Mice were euthanized according to the protocol by carbon dioxide, and for humane reasons severely ill mice were euthanized.

Genotype confirmation for MK2 and MK3 proteins. The presence or absence of MK2 and MK3 protein expression was also confirmed in the mice of all four genotypes (WT, MK2^{-/-}, MK3^{-/-}, and MK2^{-/-}MK3^{-/-}). Due to the low abundance of MK3 compared with MK2, decreased ability of anti-MK3 antibody to detect endogenous MK3, and detection of nonspecific signal by anti-MK3 antibody, total protein lysates were prepared from mouse spleens and enriched for endogenous MK2 and MK3 using recombinant GST-p38 MAPK bound to glutathione-Sepharose 4B, as previously described (41). Briefly, spleens were harvested from mice and snap frozen in liquid nitrogen and stored at -80°C until use. Frozen specimens were homogenized on ice in tissue protein extraction reagent (Thermo Scientific, Rockford, IL) in the presence of protease and phosphatase inhibitors (Sigma-Aldrich, St. Louis, MO). Lysates were centrifuged at 10,000 g for 10 min at 4°C, and the supernatants were quantified for protein concentration by a Pierce BCA protein assay kit (Pierce Biotechnology, Rockford, IL) and stored at -80°C. For GST pull-down, 1 mg of spleen lysate protein was incubated with 1.25 µg GST-p38 (Sigma-Aldrich) bound to glutathione-Sepharose 4B (GE Healthcare Life Sciences, Uppsala, Sweden) at 4°C O/N. Following three washes with immunoprecipitation buffer [mammalian protein extraction buffer (Thermo Scientific) + protease and phosphatase inhibitors + 1% Triton X-100], bound proteins were extracted from the beads in 5× SDS sample buffer and subjected to SDS-PAGE followed by Western blotting to detect MK2 and MK3 proteins, as described below.

ADR-induced nephropathy model. The ADR-induced nephropathy model was generated by injecting ADR (Sigma-Aldrich) at 18 mg/kg iv via tail vein in the male mice at 11 wk in all four genotypes (WT, MK2^{-/-}, MK3^{-/-}, and MK2^{-/-}MK3^{-/-}) of 129/SvJ mice. Twelve mice per genotype ($n = 12$) were injected with ADR, while control groups ($n = 6$) received saline injections. Urine was collected at regular intervals throughout the study by applying gentle abdominal pressure and analyzed for proteinuria on days 0, 4, 7, 14, and 21, as

described below. Mice were euthanized on days 7 ($n = 2$ ADR, $n = 2$ control; per genotype) and 21 ($n = 10$ ADR, $n = 4$ control; per genotype), and kidneys were harvested and processed as described below. A few of the ADR-injected mice exhibited serious weight loss, fatigue, and appetite loss during the course of the study, at which point they either died or were euthanized for humane reasons, and these animals were included in the mortality count for the survival analyses.

Albuminuria analyses of mouse-ADR model. As an indicator of renal injury, albuminuria was analyzed by SDS-PAGE of urine samples followed by zircon staining. Urine samples collected at days 0, 4, 7, 14, and 21 were resolved on 6–20% gradient SDS-PAGE gels. The gels were fixed (30% methanol + 7% acetic acid) for 30 min and stained (0.4% zircon + 0.3% ethyl violet in ethanol) overnight, and the albumin band densities were quantified using ImageJ (1.36u ed., National Institutes of Health, Bethesda, MD) (53). Bovine serum albumin (Sigma-Aldrich) standards at varying concentrations (0.5, 1, 1.5, and 2.5 µg) were also resolved on the gels to generate calibration curves, which were then used to calculate the absolute urinary albumin values of the unknown samples. Urinary creatinine was measured using an enzymatic creatinine assay, according to the manufacturer's instructions (Diazyme, Poway, CA). Finally, the albuminuria values were derived by normalizing the urinary albumin measurements to creatinine.

SDS-PAGE and Western blotting. Renal cortexes were harvested and snap frozen in liquid nitrogen and stored at -80°C until further use. Protein extracts were made from frozen specimens as described above and quantified. Fifteen micrograms of each protein lysate were resolved by 10% SDS-PAGE and transferred to nitrocellulose membranes. The blots were incubated in 5% nonfat milk in phosphate-buffered saline + 1% Tween 20 (PBS-T) at room temperature for 1 h for blocking. The membranes were washed with PBS-T and incubated with the primary antibody overnight at 4°C. The anti-MK2 rabbit monoclonal, anti-MK3 rabbit monoclonal, anti-p38 rabbit monoclonal, and anti-phosphorylated-HSPB1 rabbit monoclonal antibodies were purchased from Cell Signaling (Danvers, MA). The other primary antibodies used were anti-HSPB1 (StressMarq, Victoria, BC), anti-HSPB8 mouse monoclonal (Abcam, Cambridge, MA), anti-GRP78 rabbit monoclonal (StressMarq), and anti-GAPDH mouse monoclonal (Millipore, Billerica, MA). Following three washes, the membranes were incubated with appropriate horseradish peroxidase conjugated anti-mouse or anti-rabbit IgG secondary antibodies (Jackson Laboratory, Bar Harbor, ME) for 1 h at room temperature. The blots were developed with an ECL detection kit (GE Healthcare Bio-Sciences, Piscataway, NJ) and detected by exposure to X-ray film. X-ray films were scanned using a calibrated ArtixScan M1 transillumination scanner (Molecular Dynamics, Cerritos, CA) controlled by the ScanWizard Pro program (version 7.042) using standard settings. Densitometry analyses of the integrated band densities were performed using ImageJ (version 1.39, standard settings; <https://rsb.info.nih.gov/ij/>), and values were plotted using GraphPad Prism software version 6.00 for Windows.

RNA extraction and real-time quantitative RT-PCR. Total RNA was extracted from renal cortexes and used for quantitative reverse transcribed-polymerase chain reactions (qRT-PCR), as described previously (3). The frozen renal cortical tissue (snap frozen in RNA Later in liquid nitrogen) was homogenized on dry ice. The total RNA was isolated using an RNeasy kit (Qiagen, Germantown, MD) as per the manufacturer's instructions, and the concentration and purity were determined using a NanoDrop Spectrophotometer (Thermo, Wilmington, DE). One microgram of RNA was treated with DNase (Ambion, Austin, TX) at 37°C for 30 min. Following a DNase inactivation step with 5 mM EDTA at 75°C for 10 min, cDNA was synthesized in a 20-µl reaction mix using iScript reverse transcriptase (Bio-Rad Laboratories). The reaction conditions were 25°C for 5 min, 42°C for 30 min, followed by 85°C for 5 min. COX-2 and β-actin mRNAs were quantified using the SYBRGreen method on an iQ5 thermal cycler

(Bio-Rad Laboratories) as previously described (3). The primers used for COX-2 amplification were forward 5'-GATGTTTGCATTCTTTGCC and reverse 5'-GGCGCAGTTTATGTTGTCTG, and for β -actin amplification the primers were forward 5'-CTTCGTTGCCGGTCCACACCC and reverse 5'-CTGGGCCTCGTCACCCACAT. The reactions were performed at 95°C for 3 min, 40 cycles of 95°C for 10 s, and 55°C for 10 s, followed by melt curve analyses. Values were normalized to the housekeeping gene β -actin and plotted as fold changes.

Histological analyses of ADR-induced renal injury. Murine nephrectomies were bisected, fixed in 10% formalin, and paraffin embedded ($n = 3$ for each group). Three-micrometer whole mount sections were stained with hematoxylin and eosin and periodic acid-Schiff stain. The slides were examined and scored by an expert renal pathologist in a blinded fashion. Each specimen included at least 100 glomeruli. Each specimen was assigned a semiquantitative pathology score (0–3) for the glomerular compartment including mesangial cellularity (M0, no mesangial hypercellularity or 8 mesangial cells/mesangial area), glomerular sclerosis (A, segmental glomerular sclerosis; B, global glomerular sclerosis), mesangiolysis (absent or present), and extracapillary proliferation (F, focal or >50% glomerular involvement). Additional features of cellular vacuolization, karyorrhectic debris, and exudative lesions were recorded but not scored. Tubular features (dilatation/microcysts, protein reabsorption droplets, cytoplasmic vacuolization, casts, and atrophy) and interstitial changes (fibrosis 0 and 50% and inflammation) were graded. Vascular changes (myocyte vacuoles and sclerosis) were recorded if present.

Puromycin aminonucleoside-induced nephropathy model. The performed studies were approved by the Institutional Animal Care and Use Committee at Nationwide Children's Hospital, and all the experiments were performed in accordance with the approved guidelines. Proteinuria was induced in male Sprague-Dawley rats weighing ~150–200 g by single intravenous puromycin aminonucleoside (PAN; Sigma-Aldrich) injection (75 mg/kg) on *day 0*, while the control group received intravenous saline injections ($n = 11$). A group of PAN-injected rats ($n = 13$) were left untreated and received sham oral gavage vehicle solution (0.5% methylcellulose and 0.025% Tween 20), while the treatment group ($n = 14$) also received PF-318 (kind gift from Pfizer) at 30 mg/kg b.i.d. by oral gavage daily. The treatment control group ($n = 14$) received PF-318 alone (30 mg/kg b.i.d.) by oral gavage daily with no PAN injection. Urine samples were collected at baseline (before injury) and daily during the study for analysis. The rats were weighed daily and euthanized on *day 21* at the point of expected proteinuria remission, and the kidneys were harvested.

Urine analyses of rat-PAN model. Albuminuria was monitored by analyzing 4- μ l urine samples taken at *days 0, 2, 4, 7, 9, 11, 14, 18, and 21* for the presence of albumin by SDS-PAGE and Zincon. Urine protein-to-creatinine ratios (UPC) were measured at *day 11* (expected peak proteinuria) by Antech Diagnostics Good Laboratory Practice (Morrisville, NC), which is fully compliant with Good Laboratory Practice regulations as previously reported (2).

Statistical analyses. Statistical significance was determined by one-way or two-way ANOVA for multiple group comparisons using the GraphPad Prism software version 6.00 for Windows. $P < 0.05$ was considered significant. Albuminuria graphs were prepared from $n = 10$ mice/group, and Western and qRT-PCR experiments were performed in at least $n = 3$ mice/group. Proteinuria graphs were prepared from *day 11* UPC values from rats. Data are shown as either representative blots or as means \pm SE. Survival analysis was plotted, and curve comparison was performed using log-rank (Mantel-Cox) and Wilcoxon tests using the GraphPad Prism software version 6.00 for Windows.

RESULTS

Generation and validation of MK2/MK3 knockout mice in ADR-susceptible background. Various genotypic combinations of MK2/MK3 KO mice in Sv129 background were generated by backcrossing double heterozygous mice (MK2^{+/-}MK3^{+/-}) in C57BL/6 background with WT 129/SvJ mice for seven generations, as described in MATERIALS AND METHODS. The amplicons corresponding to MK2-WT and MK2-KO alleles were 200 and 560 bp, and amplicons corresponding to MK3-WT and MK3-KO alleles were 879 bp and 1,239 bp, respectively (Fig. 1A). Thus all four genotypes (WT, MK2^{-/-}, MK3^{-/-}, and MK2^{-/-}MK3^{-/-}) of mice were successfully generated in enough numbers for the subsequent studies ($\geq n = 18$ /genotype).

The presence and absence of MK2 and MK3 proteins in their respective WT and KO genotypes were also confirmed at the protein level using anti-MK2 and anti-MK3 antibodies, as previously described (41). The untreated lysates (Fig. 1B, input) showed specific MK2 bands but nonspecific MK3 bands, due to low levels of expression of MK3 and some nonspecificity of the anti-MK3 antibodies. Thus the spleen

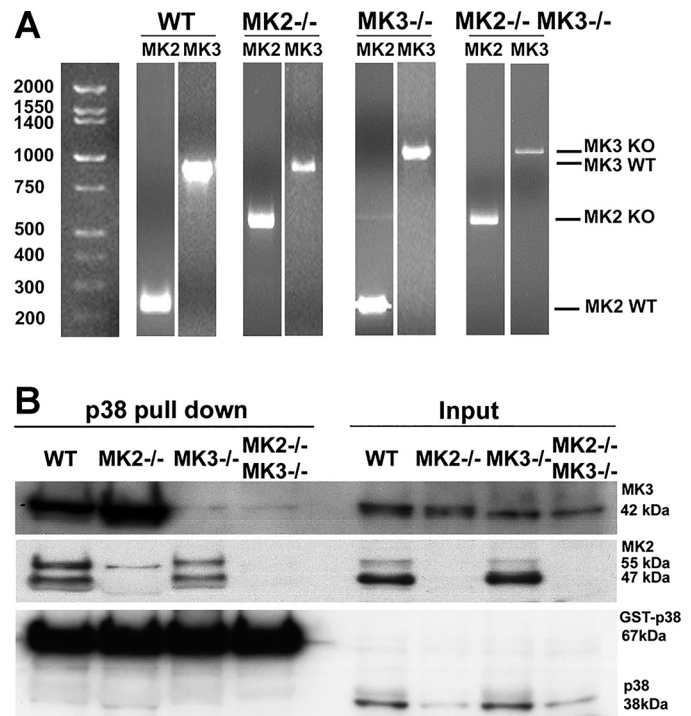


Fig. 1. Generation and validation of MK2/MK3 knockout (KO) mice in an adriamycin (ADR)-susceptible background. MK2/MK3 heterozygous mice in C57BL/6 background were backcrossed with 129/SvJ for 7 generations to obtain MK2, MK3 and MK2/MK3 KO mice in ADR-susceptible strain. A: genotyping by PCR is shown for representative mice for all the 4 genotypes. The amplicons corresponding to MK2-wild type (WT) and MK2-KO alleles were 200 and 560 bp. The amplicons corresponding to MK3-WT and MK3-KO alleles were 879 and 1,239 bp. B: the absence and presence of MK2 and MK3 in their respective KO and WT genotypes were confirmed by Western blotting. MK2 and MK3 were precipitated by GST-p38 bound to glutathione-Sepharose 4B before detection with their respective antibodies. Left 4 lanes (p38 pull down): MK2 and MK3 were precipitated from spleen lysates by GST-p38 bound to glutathione-Sepharose 4B and detected by respective antibodies. Right 4 lanes (input): unprecipitated input lysates. The untreated lysates (input) showed specific MK2 bands but nonspecific MK3 bands that were cleared by GST-p38 precipitation.

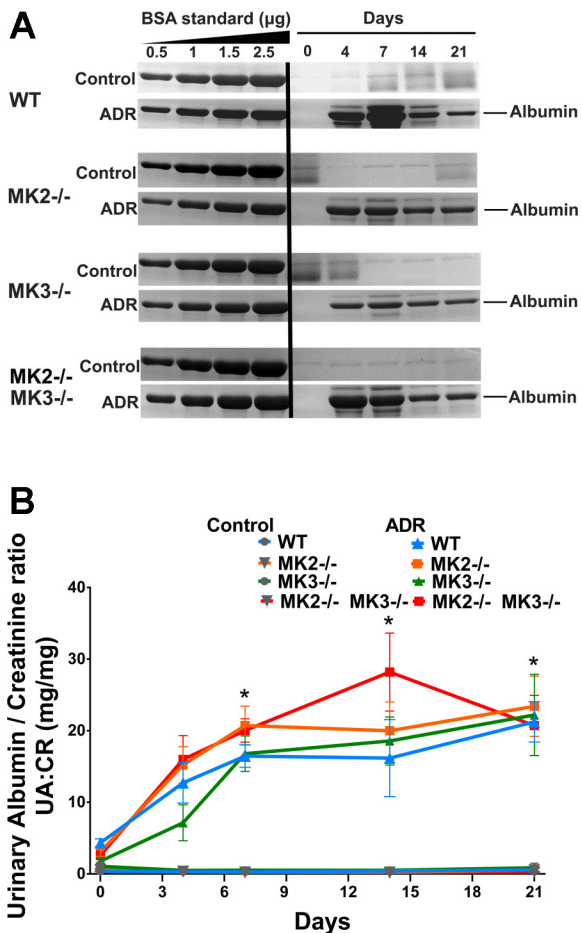


Fig. 2. ADR injection induced massive proteinuria in WT and MK2/MK3 KO Mice. Albuminuria was induced in male mice of all 4 genotypes by single intravenous ADR injections (18 mg/kg) on day 0. A: representative gels of urinary albumin as visualized on zircon-stained SDS-PAGE gels. Urines were collected daily, and equal volumes (control × μl, ADR-treated μl) from selected days were analyzed. BSA standard were run at 0.5, 1, 1.5, and 2.5 μg for albumin quantitation. B: urinary albumin/creatinine ratios (UA:CR) are plotted through the course of the experiment. Statistical differences are indicated as * *P* < 0.05, control vs. ADR as determined by two-way ANOVA Tukey's multiple comparison test.

lysates from these mice were first cleared and enriched for p38 MAPK-bound proteins (MK2 and MK3) using GST-p38 bound to glutathione-Sepharose 4B before detection. MK2 (47 and 55 kDa) could be detected in WT and MK3^{-/-} but not in MK2^{-/-} and MK2^{-/-}MK3^{-/-} mice (Fig. 1B). Specific MK3 bands (42 kDa) could be detected in WT and MK2^{-/-} but not in (MK3^{-/-} and MK2^{-/-}MK3^{-/-}) mice (Fig. 1B). Thus the

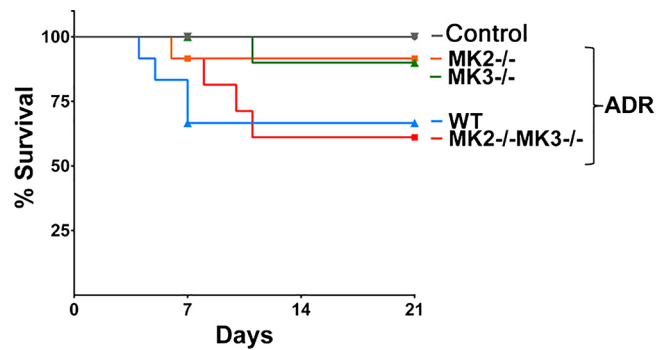


Fig. 3. ADR-induced toxicity was not significantly different among the 4 genotypes. Survival plot was generated for all the genotypes injected with ADR. At 11 wk of age, male mice from each genotype (WT, MK2^{-/-}, MK3^{-/-}, and MK2^{-/-}MK3^{-/-}) were injected with 18 mg/kg ADR (ADR group, *n* = 12 each genotype) or PBS (control group, *n* = 6 each genotype) by tail vein injections. At days 7 and 21, 2 and 10 mice, respectively, were killed and included in the survival analyses.

complete absence of MK2 and MK3 protein expression was confirmed in their respective KO genotypes.

ADR-injection induced massive proteinuria in WT and MK2/MK3 knockout mice. Albuminuria as a functional indicator of ADR-induced NS was analyzed in all four genotypes of mice and compared with the PBS-treated control groups. The baseline (day 0) urinary albumin-to-creatinine ratio (UA:CR) was negligible and did not change with either MK2 or/and MK3 gene deletion (Fig. 2, A and B). Upon ADR injection, albuminuria was observed across all four genotypes, which started at day 4 and progressively worsened to day 21, with ~25-fold increases (Fig. 2, A and B). Although the severity of albuminuria was not dramatically different among the different genotypes, there were some minor but noticeable differences (Table 1). MK2^{-/-} and MK2^{-/-}MK3^{-/-} mice were the earliest to show albuminuria upon ADR injection (on day 4) compared with untreated mice of the same genotypes, suggesting some potential importance of MK2. In contrast, the WT and MK3^{-/-} did not display significant albuminuria at day 4 compared with their respective controls, and only began to develop significant albuminuria starting at day 7. Moreover, albuminuria levels in MK2^{-/-} mice were found to display the highest levels of significance at days 7, 14, and 21 compared with the other genotypes (Table 1).

ADR-induced toxicity was not significantly different among the MK2 and MK3 genotypes. Survival analyses revealed that the WT mice showed a trend toward more severe ADR-induced toxicity compared with controls, with 65% survival by day 21 (Fig. 3). Notably, while similarly reduced survival was

Table 1. Albuminuria severity among MK2 and MK3 genotypes upon adriamycin treatment

Days	Genotype			
	WT	MK2 ^{-/-}	MK3 ^{-/-}	MK2 ^{-/-} MK3 ^{-/-}
0	(0.36 ± 0.11) vs. (4.35 ± 0.55)	(0.60 ± 0.17) vs. (3.11 ± 0.66)	(1.05 ± 0.61) vs. (1.78 ± 0.33)	(0.47 ± 0.17) vs. (2.59 ± 0.60)
4	(0.29 ± 0.07) vs. (12.72 ± 2.82)	(0.30 ± 0.05) vs. (15.21 ± 2.56)*	(0.50 ± 0.18) vs. (7.14 ± 2.51)	(0.34 ± 0.17) vs. (15.99 ± 3.33)*
7	(0.27 ± 0.03) vs. (16.45 ± 1.57)*	(0.24 ± 0.10) vs. (20.71 ± 2.71)***	(0.52 ± 0.25) vs. (16.80 ± 2.48)**	(0.17 ± 0.08) vs. (20.04 ± 1.62)**
14	(0.43 ± 0.12) vs. (16.18 ± 5.38)*	(0.23 ± 0.11) vs. (20.00 ± 4.01)***	(0.50 ± 0.43) vs. (18.56 ± 3.35)**	(0.13 ± 0.07) vs. (28.20 ± 5.44)****
21	(0.55 ± 0.10) vs. (21.23 ± 2.82)***	(0.55 ± 0.34) vs. (23.41 ± 4.21)****	(0.86 ± 0.65) vs. (22.20 ± 5.67)***	(0.22 ± 0.13) vs. (20.73 ± 4.20)***

Values are means ± SE of urinary albumin-to-creatinine ratios for control vs. adriamycin (ADR)-treated mice. WT, wild type. **P* < 0.05; ***P* < 0.01; ****P* < 0.001; *****P* < 0.0001.

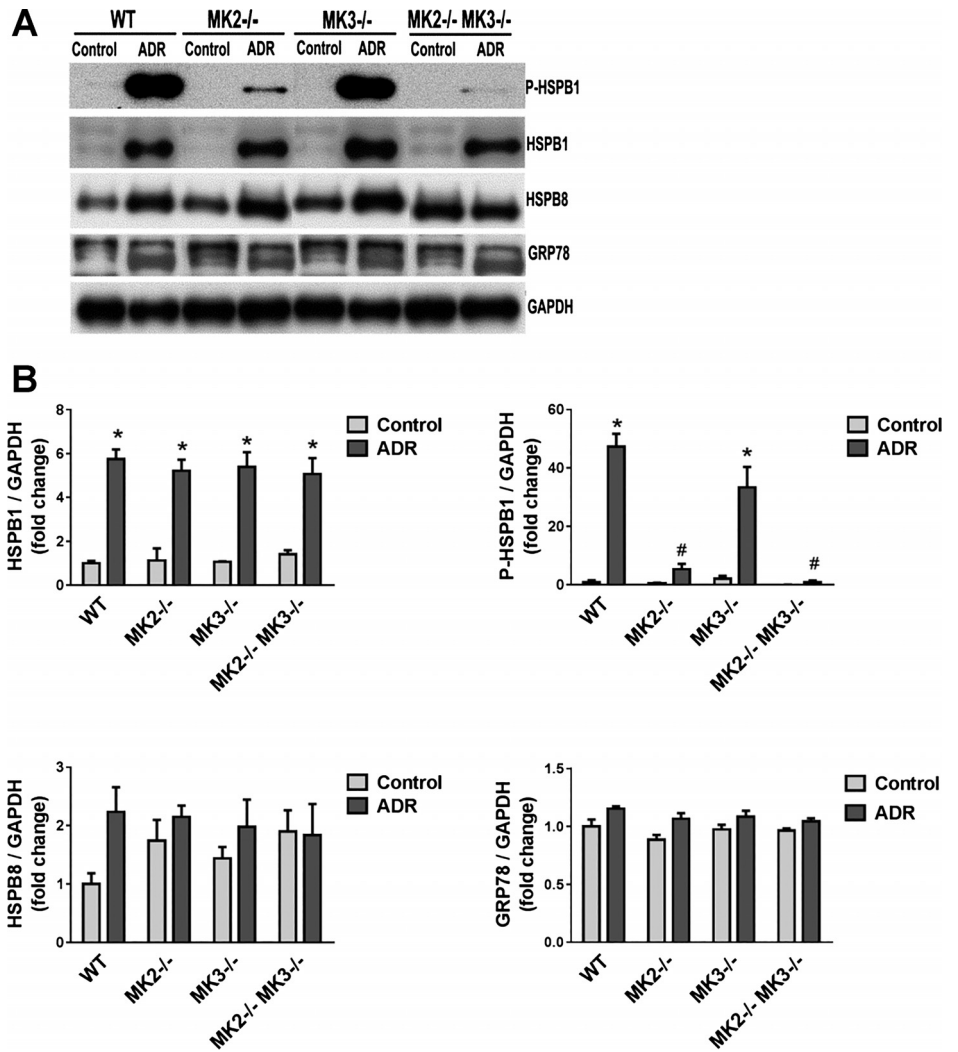


Fig. 4. ADR-induced injury induced and activated small heat shock proteins (HSPs), primarily in an MK2-dependent manner. Total protein was extracted from renal cortexes isolated from control and ADR-injured mice on day 21 from each genotype and phosphorylated and total forms of HSPB1, HSPB8, glucose-regulated protein 78 (GRP78), and GAPDH were detected using their respective antibodies. A: representative Western blots of total and phosphorylated forms of selected proteins. B: densitometry analyses of protein induction/phosphorylation in the renal cortexes of at least 3 mice from each genotype. Statistical differences: **P* < 0.05, control vs. ADR; #*P* < 0.05, WT-ADR treated vs. KO-ADR treated.

seen in the MK2^{-/-}MK3^{-/-} mice, both of the single KO groups (MK2^{-/-} and MK3^{-/-}) showed trends toward increased survival, with 90% survival at day 21 (Fig. 3). However, none of these trends were statistically significant.

ADR-induced injury induced and activated sHSP, primarily in an MK2-dependent manner. Induction and activation of proteins involved in stress responses, including the sHSPs HSPB1 and HSPB8 and another HSP HSPA5/GRP78, were studied during ADR-induced nephropathy in all four genotypes. HSPB1 gene expression was highly induced in all four genotypes (WT, MK2^{-/-}, MK3^{-/-}, and MK2^{-/-}MK3^{-/-}) in ADR-injected mice (Fig. 4, A and B). Moreover, HSPB1 was significantly activated (as measured by its phosphorylation) by ADR injection in WT and MK3^{-/-} mice but not in either the MK2^{-/-} or the MK2^{-/-}MK3^{-/-} mice. Furthermore, ADR induced HSPB8 expression modestly (but not significantly) in WT mice, despite less or no induction in the other genotypes, while GRP78 remained unaltered with injury in all genotypes (Fig. 4, A and B).

ADR-induced injury induced COX-2 in an MK2-dependent manner. The renal cortical expression of COX-2 in all four genotypes of ADR-injured mice was also studied, as increased COX-2 expression has been previously linked to podocyte

injury in a p38 MAPK- and MK2-dependent manner (3, 38). COX-2 gene expression was significantly reduced in untreated MK2^{-/-}, MK3^{-/-}, and MK2^{-/-}MK3^{-/-} groups compared with WT (Fig. 5). Furthermore, although COX-2

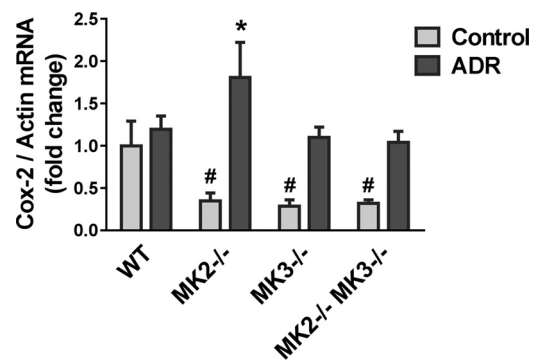


Fig. 5. ADR-induced injury induced cyclooxygenase-2 (COX-2) in an MK2-dependent manner. Total RNA was extracted from the renal cortexes isolated from control and ADR-injured mice on day 21 from each genotype (*n* = 3 per genotype). Relative mRNA levels of COX-2 was measured by quantitative RT-PCR and normalized to GAPDH. Statistical differences: **P* < 0.05, control vs. ADR. #*P* < 0.05, WT vs. KO.

was not significantly induced in WT mice upon ADR injury, it was significantly induced (~3 fold) in the ADR-injected MK2^{-/-} group, with lesser inductions in the MK3^{-/-} and MK2^{-/-}MK3^{-/-} groups (Fig. 5).

ADR induced renal injury in all four genotypes in MK2- and MK3-dependent manner. Analysis of WT-control murine kidney (Fig. 6, A and B, and Table 2) revealed rare mild mesangial hypercellularity (M1) and rare segmental karyorrhectic debris. No significant glomerular extracapillary proliferation, no tubular abnormalities, no interstitial fibrosis, and no vascular changes were identified.

ADR-treated WT murine kidneys had foci of mesangioly-sis (Fig. 6C and Table 2) and foci of exudative lesions (Fig. 6D), and focal mild mesangial hypercellularity (Fig. 6E) with rare focal segmental tuft sclerosis. Diffuse extracapillary hypertrophy with occasional cytoplasmic vacuoles (Fig. 6E) was also present. Small tubular hyaline luminal contents with occasional dilatation, foci of tubular epithelial protein reabsorption droplets (Fig. 6F), and foci of diffuse moderate to severe acute tubular epithelial cell injury were present. Additionally, myocyte vacuoles were also present.

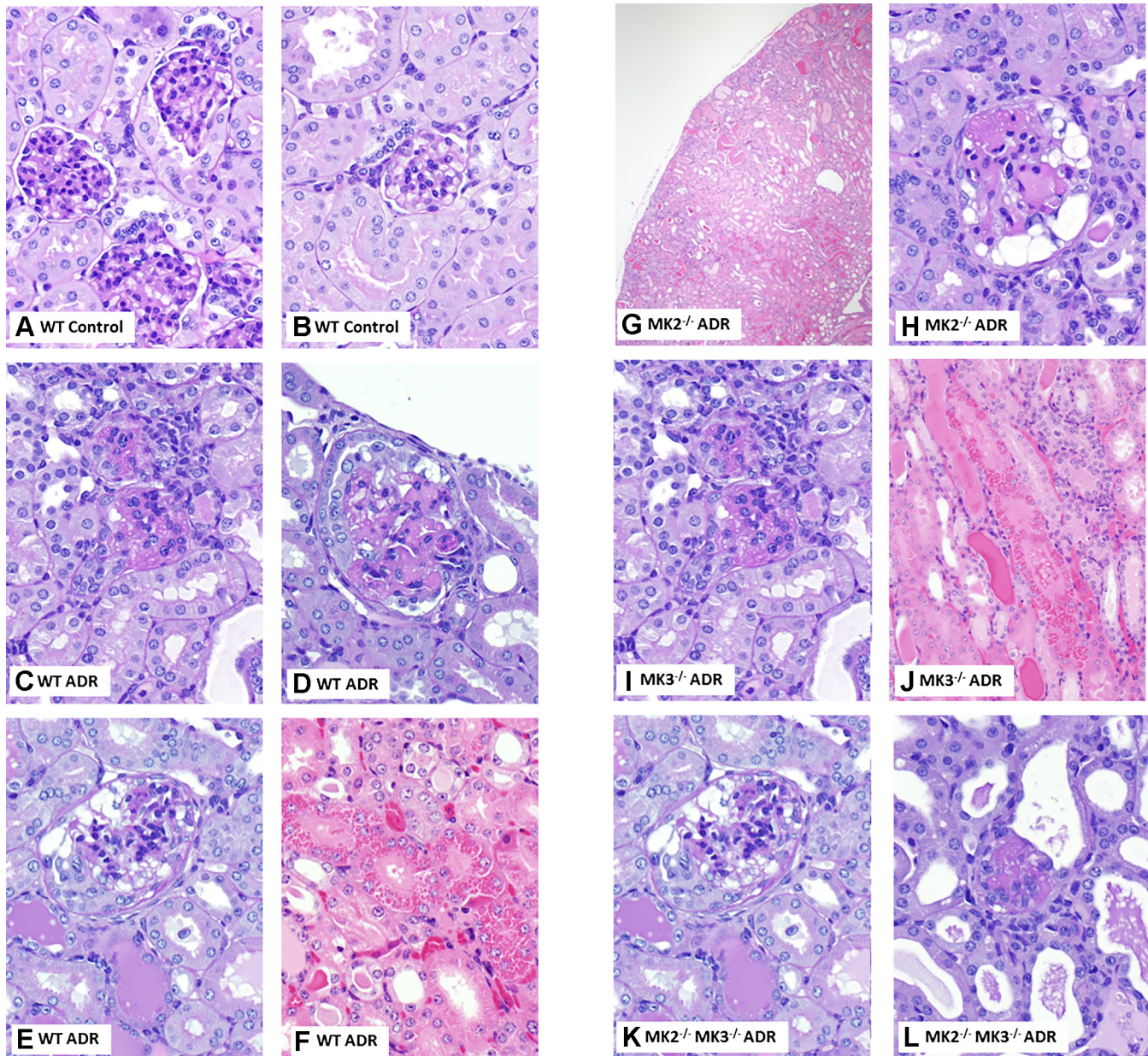


Fig. 6. ADR induced renal injury in all four genotypes in MK2 and MK3-dependent manner. Representative images of WT control (A and B) [periodic acid-Schiff (PAS) at $\times 40$]; ADR-treated WT mesangioly-sis (PAS at $\times 40$; C); ADR-treated WT mesangioly-sis, exudative lesions, and podocyte hypertrophy (PAS at $\times 40$; D); ADR-treated WT mesangial hypercellularity and cytoplasmic vacuoles (PAS at $\times 40$; E); ADR-treated WT tubular epithelial cell protein reabsorption droplets [hematoxylin and eosin (H&E), $\times 40$; F]; ADR-treated MK2^{-/-} tubular microcysts and hyaline casts (H&E at $\times 4$; G); ADR-treated MK2^{-/-} segmental sclerosis and cytoplasmic vacuolization (PAS at $\times 40$; H); ADR-treated MK3^{-/-} moderate mesangial hypercellularity and podocyte hypertrophy (PAS at $\times 40$; I); ADR-treated MK3^{-/-} tubular epithelial cell protein reabsorption droplets and hyaline casts (H&E at $\times 40$; J); ADR-treated MK2^{-/-}MK3^{-/-} segmental sclerosis (PAS at $\times 40$; K); and ADR-treated MK2^{-/-}MK3^{-/-} global glomerular sclerosis (PAS at $\times 40$; L).

Table 2. Renal histopathology scoring sheet

Genotype/ADR/mouse ID#	Intracapillary (≥4)/glomerular		Tubules								
	Hypercellularity 0, 1, 2, 3	Sclerosis: A = segmental B = global Matrix: M0-M3	Extracapillary /crescent	Dilatation	Droplets /vacuoles	Casts	AKI	Atrophy	IFTA	Vascular sclerosis	Deposits (IF)
WT without ADR											
1006	0	Karyorrhectic debris F	0	—	—	—	—	—	0	0	N/A
1007	0	—	0	—	—	—	—	—	0	0	N/A
1008	M1 F	Karyorrhectic debris F	0	—	Hyaline F	—	—	—	0	0	N/A
WT with ADR											
861	0	Mesangiolysis; exudative lesions	Extracapillary D		Hyaline	Granular F; hyaline microcyst D	3	—	0	Myocyte vacuoles	N/A
866	M1 F	Mesangiolysis; exudative lesions	Extracapillary D with vacuolization D		Hyaline	Hyaline microcyst D	2	—	0	Rare myocyte vacuoles	N/A
869	M1 F	Mesangiolysis; exudative lesions; Scl A (rate = 1)	Extracapillary D with vacuolization D		Hyaline D	Hyaline microcyst D	2	—	0	Rare myocyte vacuoles	N/A
MK2 ^{-/-} with ADR											
1155	M1 F	Mesangiolysis; exudative lesions; karyorrhectic debris F; Scl A	Extracapillary D with (macro) vacuolization D		Vacuolization	Granular F; hyaline microcyst D	1	—	0	0	N/A
1481	M1 F	Mesangiolysis; exudative lesions; Scl A	Extracapillary D with (macro) vacuolization D		Vacuolization	Granular F; hyaline microcyst D	1	—	0	0	N/A
1571	M1 F	Karyorrhectic debris D; mesangiolysis; exudative lesions; Scl A	Extracapillary D with (macro) vacuolization D		hyaline	Granular F; hyaline microcyst D	3; Karyorrhectic debris F	—	0	0	N/A
MK3 ^{-/-} with ADR											
1056	M2 F	Mesangiolysis; exudative lesions; Scl A	Extracapillary D with vacuolization D		Hyaline	Hyaline microcyst D	1	—	0	0	N/A
1604	M1 F	Exudative lesions; Scl A	Extracapillary D with vacuolization D		hyaline	Hyaline microcyst D	—	—	0	0	N/A
1631	M2 F	Scl A	Extracapillary D with vacuolization D		Hyaline	Hyaline microcyst D	Karyorrhectic debris F	—	0	0	N/A
MK2 ^{-/-} /MK3 ^{-/-} with ADR											
1040	M2 F	Mesangiolysis; Scl A	Extracapillary D with vacuolization D		Hyaline	Hyaline microcyst D	—	—	0	0	N/A
1141	M2 F	Scl A; Scl G	Extracapillary D with vacuolization D		Hyaline	Hyaline microcyst D	—	—	0	0	N/A
1582	M2 F	Scl A; Scl G	Extracapillary D with vacuolization D		Hyaline	Granular F; hyaline microcyst D	1	—	0	0	N/A

Murine kidney scoring sheet > 100 glomeruli per sample. Scoring based on Ref. 8a.: 0 = no change; 1 = mild (<25%); 2 = moderate (25–50%); and 3 = severe (>50%). I, interstitial fibrosis; IFTA, interstitial fibrosis and tubular atrophy; AKI, acute kidney injury; Scl, sclerosis; F, focal; D, diffuse; M, mesangial matrix expansion (note: not in original article).

Both ADR-treated MK2^{-/-} and MK3^{-/-} groups both had diffuse mesangiolysis and diffuse exudative lesions (Fig. 6, G–J, and Table 2). Mild mesangial hypercellularity (M1) was present in both with foci of moderate mesangial hypercellularity (Fig. 6I) in the MK3^{-/-} ADR group. Segmental glomerular sclerosis was present in all samples, with prominent diffuse extracapillary hypertrophy with often large cytoplasmic vacuolization (Fig. 6H). Diffuse tubular dilatation with microcystic change (Fig. 6G), frequent hyaline casts (Fig. 6, G and J), and tubular epithelial protein reabsorption droplets (Fig. 6J) was pronounced.

ADR-treated MK2^{-/-}MK3^{-/-} group exhibited diffuse moderate mesangial hypercellularity (M2), frequent segmental tuft sclerosis (Fig. 6K), as well as foci of global glomerular sclerosis (Fig. 6L and Table 2). Extracapillary hypertrophy with large cytoplasmic vacuolization was pronounced. Diffuse tubular dilatation with microcystic change, frequent hyaline casts, and tubular epithelial protein reabsorption droplets was also pronounced. No vascular abnormalities were identified.

MK2 inhibition with PF-318 did not significantly reduce PAN-induced proteinuria in rats. Sprague-Dawley rats developed massive proteinuria after a single intravenous PAN injection of 75 mg/kg ($n = 13$), which peaked on day 11 (UPC: 39.7 ± 5.5 mg/mg; Fig. 7, A and B). The control rats received IV saline with drug vehicle by oral gavage ($n = 11$) and maintained baseline levels of urinary protein (UPC: 1.6 ± 0.2 mg/mg). To analyze the ability of the MK2 inhibitor PF-318 to reduce PAN-induced proteinuria, 14 rats/group were also treated with twice daily oral gavage administration of PF-318 (30 mg/kg), which showed a trend toward proteinuria reduction but did not result in a significant reduction (29%, $P = NS$ vs. PAN; UPC: 28.1 ± 3.8 mg/mg) (Fig. 7, A and B). Administration of PF-318 alone ($n = 14$) did not alter the baseline urinary protein (UPC: 1.7 ± 0.2 mg/mg) but was found to be toxic when given alone to rats, with 50% mortality seen by day 14 (Fig. 7C). In summary, direct inhibition of MK2 with PF-318 was not able to induce a significant reduction in PAN-induced proteinuria and was found to be toxic when given alone to healthy rats.

DISCUSSION

This study was designed to test the hypothesis that the downstream targets of p38 MAPK, MK2, and/or MK3, play an important role in mediating injury in experimental NS via their actions on their downstream substrates HSPB1 and COX-2. To test this hypothesis, we examined the effects of both pharmacological and genetic inhibition of MK2 and MK3 in PAN-induced and in ADR-induced nephropathy in rats and mice, respectively. Using various genotypes of mice with MK2 and/or MK3 deleted, we found that genetic deletion of MK2 and/or MK3 did not alter baseline renal function and that ADR induced generally similar massive proteinuria in mice with or without MK2 and/or MK3 deleted. Furthermore, we found that ADR-induced injury resulted in significant cortical induction of the HSPB1 in all genotypes, with additional activation (i.e., phosphorylation) of HSPB1 only in the genotypes WT for its major upstream kinase, MK2 (i.e., WT and MK3^{-/-} mice). Moreover, COX-2 was significantly reduced in untreated MK2^{-/-}, MK3^{-/-}, and MK2^{-/-}MK3^{-/-} groups compared with WT and while ADR injury did not significantly induce

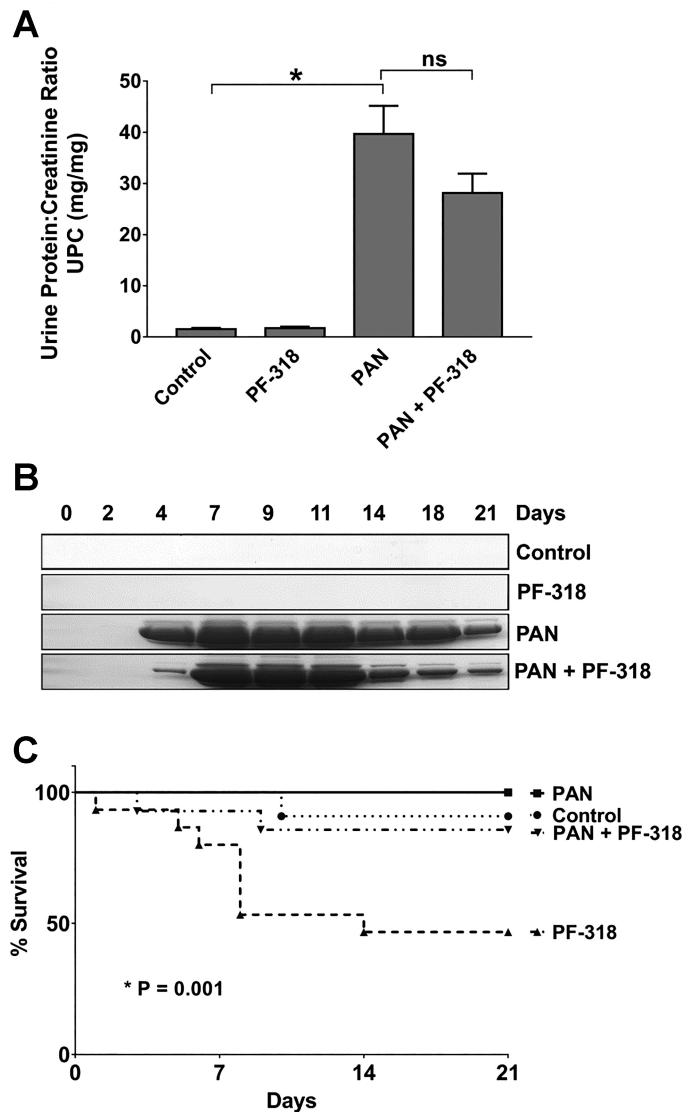


Fig. 7. Specific pharmacologic MK2 inhibition with PF-318 did not significantly reduce puromycin aminonucleoside (PAN)-induced proteinuria in rats. Proteinuria was induced in male Sprague-Dawley rats by single intravenous PAN injections (75 mg/kg) on day 0 ($n = 13$). The PAN + PF-318 treatment group ($n = 14$) also received twice daily oral gavage administration of the specific MK2 inhibitor PF-318 (30 mg/kg). Control rats received intravenous saline with drug vehicle by oral gavage ($n = 11$). PF-318 control rats received twice daily oral gavage administration of PF-318 (30 mg/kg) without disease induction for 10 days. **A**: urine protein/creatinine ratios (UPC) are plotted on day 11 of the experiment (date are means \pm SE; * $P < 0.05$; determined by one-way ANOVA Tukey's multiple comparison test). **B**: representative gels depicting albuminuria after PAN injection and treatment with PF-318. Urines were collected daily and equal volumes (4 μ l) from selected days were analyzed by SDS-polyacrylamide gel electrophoresis and Zincon staining. **C**: a survival plot was generated for all the treatment groups of Sprague-Dawley rats. All the rats were killed on day 21. PF-318 treatment alone induced significant toxicity (as measured by log-rank (Mantel-Cox) test and Wilcoxon test).

renal cortical COX-2 in WT mice, COX-2 was clearly induced by ADR in mice with MK2 deleted, as well to a lesser extent in mice with MK3 or both MK2 and MK3 deleted. Additionally, in an acute model of PAN-induced NS in rats, a specific small molecule inhibitor of MK2, PF-318, was unable to provide beneficial proteinuria-reducing effects and instead im-

parted toxic effects when administered alone to the rats. Together, these data suggest that while the inhibition of MK2 and/or MK3 regulates the renal stress response, our currently available approaches are not yet able to safely and effectively reduce proteinuria in experimental NS and that other p38 MAPK downstream targets should also be considered to improve the future treatment of glomerular disease (see Fig. 8).

FSGS is one of the most common acquired glomerular diseases leading to end-stage kidney disease (24, 25, 29), and its incidence is rising around the world in virtually all ethnic and age groups (6). Moreover, currently available therapies for NS, including glucocorticoids, have many side effects are generally ineffective in FSGS, which often relapses (20~25%) after kidney transplantation (24, 25, 29). Therefore, there is an urgent and unmet medical need to develop safe and effective therapies for NS, including FSGS. To this effect, recent reports have indicated the importance of p38 MAPK as a potential therapeutic target for NS and FSGS (30), and a proof-of-concept clinical trial has been undertaken using the p38 MAPK inhibitor Losmapimod in patients with FSGS (<https://clinicaltrials.gov/ct2/show/NCT02000440>). p38 MAPK is a major protein kinase and is involved in a diverse range of biological functions, including differentiation, proliferation, inflammation, apoptosis, cytoskeletal regulation, and fibrosis (19, 34). It is induced and activated in multiple cell types in response to extracellular stimuli, stress, proinflammatory cytokines, and many other triggers and thus plays an essential role in the mediation of cellular responses to these events (18). Dramatic increases in p38 MAPK activation in glomeruli, podocytes, glomerular endothelial cells, infiltrat-

ing macrophages, neutrophils, tubular epithelial cells, and myofibroblasts have been reported in several experimental models of NS and glomerulonephritis (30, 51, 56). In podocytes, high glucose exposure has been shown to stimulate p38 MAPK phosphorylation and collagen expression (28). p38 MAPK activation has also been shown to correlate with glomerular disease, as well as with the degree of proteinuria and glomerular injury (30, 52). Moreover, inhibition of p38 MAPK in experimental models has been reported to reduce proteinuria in NS and glomerulonephritis, ameliorate renal ischemia, and reduce reperfusion injury (16, 30, 56). However, attempts to utilize p38 MAPK inhibitors in clinical trials for many diseases have been unsatisfactory, due to their significant side effects (15, 18). Therefore, we previously analyzed the potential utility of targets downstream of p38 MAPK in both podocytes (38) and in experimental acute glomerulonephritis (20). In the present report, we have extended these studies to analyses of such targets using both genetic and pharmacologic approaches in rodent models of chronic and acute NS, respectively.

p38 MAPK has diverse downstream targets, including the first identified MAPK-activated protein kinases MK2 and MK3 as direct substrates of p38 MAPK (10, 41, 48). MK2 and MK3 are often referred to as phylogenetically related protein kinases, as they share 75% share homology in their structure, and they also share similar downstream effectors (42). Although MK2 is the predominant kinase, they contribute to similar cellular functions such as endocytosis, migration, cytoskeletal reorganization, chromatin remodeling, cytokine production, transcriptional regulation, and cell cycle control (19, 21, 41,

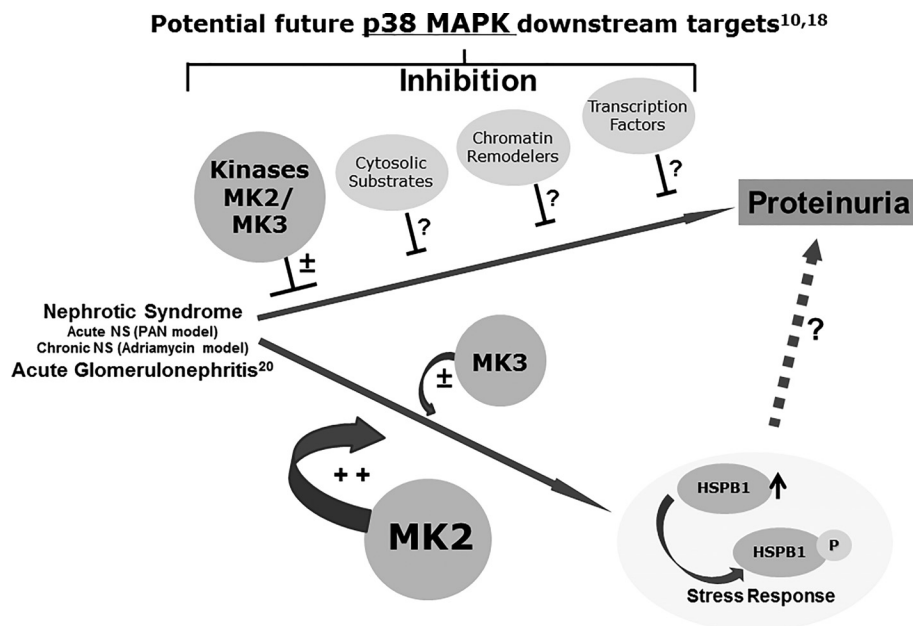


Fig. 8. Schematic summarizing and depicting the roles of MK2 and MK3 in regulating stress response and proteinuria during nephrotic syndrome nephrotic syndrome induction in experimental rodent models resulted in massive proteinuria. Genetic deletion of MK2 and MK3 did not impart any clear proteinuria reducing effects in ADR-induced nephrotic syndrome (NS) in mice. Similarly, specific pharmacological MK2 inhibition also did not result in significant proteinuria reducing effects in PAN-induced NS. We previously reported similar nonbeneficial effects of MK2 and MK3 deletion in acute proliferative glomerulonephritis model in mice (20). Interestingly, we found that ADR injury resulted in massive renal cortical induction of the sHSPs HSPB1 and HSPB8, while HSPB1 was also significantly phosphorylated and activated only in the genotypes WT for MK2 (WT and MK3^{-/-}) and only very mildly activated in the genotypes deleted for MK2 and WT for MK3 (MK3^{-/-} and MK2^{-/-}MK3^{-/-}). These results suggest that while MK2 and MK3 inhibition may not induce clear reductions in proteinuria during NS, MK2, and not MK3, plays an important role in mediating the renal stress response in a chronic model of NS. Together, these and our previous preclinical studies suggest that our currently available approaches are not yet able to safely and effectively reduce proteinuria in experimental NS and that other p38 MAPK downstream targets (i.e., other cytosolic substrates, chromatin remodelers, and transcription factors) (10, 18) should also be considered to improve the future treatment of glomerular disease.

46, 58). MK2 and MK3 are activated by different stress signals such as an altered oxidative state, heat shock, hyperosmolarity, and LPS treatment (41, 43). Moreover, both of these kinases are essential for production of several inflammatory cytokines, with roles in the posttranscriptional regulation of proinflammatory gene expression (13, 44). However, under different pathological conditions, MK2 and MK3 have been reported to exhibit distinct functions (32, 41). These studies showed that while MK3 KO mice did not have any notable changes in inflammatory response upon LPS stimulation, MK2 KO mice produced less TNF α and IL-6, which was further reduced in MK2/3 double KO mice. These findings indicated that the inflammatory response downstream of MK2 is also influenced by MK3. MK2 has also been shown to be a key player in systemic autoimmune inflammatory disease, since MK2 KO mice exhibited greater resistance to collagen-induced rheumatoid arthritis than WT (23). Compared with MK2, MK3 shows delayed cytosolic translocation, and its export is independent of the activation state (57). Moreover, distinct from MK2, MK3 has an inhibitory ability in the development of IFN- γ mediated innate and adaptive immune responses (31). Furthermore, we have found that MK2 is crucial in *in vitro* models of podocyte injury, while MK2 and MK3 together play crucial roles in the regulation of the renal stress response in an experimental model of acute proliferative glomerulonephritis (20, 38). Surprisingly, in the present studies we did not observe significant crucial differences in proteinuria and renal function (data not shown) among MK2 and/or MK3 KO vs. WT mice in a chronic model of ADR-induced NS, despite observing distinct functional activities of MK2 and MK3 in regulating the renal stress response to injury. While extensive pathological changes such as mesangiolysis, focal segmental sclerosis, and extracapillary hypertrophy were observed in WT mice treated with ADR as compared with control, ADR induced generally similar renal lesions in mice with or without MK2 and/or MK3 deletion. Additionally, MK2 or MK3 deletion resulted in increased segmental glomerular sclerosis and the double deletion of both MK2 and MK3 showed frequent segmental tuft sclerosis as well as foci of global sclerosis. These data are in accordance with the inability of either the inhibition of MK2 and/or MK3 in reducing proteinuria in the presently studied chronic model of ADR-induced NS. Similarly, MK2 inhibition did not significantly reduce proteinuria in an acute model of PAN-induced NS.

ADR-induced nephropathy in mice and rats is an established and robust model that mimics human FSGS and is characterized by massive proteinuria and glomerular structural changes (40, 60). Moreover, some strains of mice are more susceptible to ADR than others, with 129/Sv mice being highly susceptible to ADR, resulting in early onset of proteinuria and progression to significant glomerulosclerosis, and C57BL/6 mice being relatively resistant to disease induction (40, 59, 60). In the present study we backcrossed MK2/3 KO in 129/Sv background for seven generations to render them ADR-susceptible. Unfortunately, we did not observe any noticeable significant reductions in proteinuria in MK2/3 KO mice compared with WT mice. However, since the ADR-induced NS model is a robust FSGS model resulting in massive proteinuria and sometimes even toxicity in mice, it may not be sensitive enough to observe any subtle potentially beneficial effects due to MK2/3 deletions. Therefore, we extended our experiments to a more sensitive and transient model of NS in rats by using a small molecule inhibitor of MK2, PF-318 (4, 5,

14, 37). Although PF-318 treatment resulted in a trend toward proteinuria reduction, the difference was not significant and the inhibitor itself exhibited toxicity, with 50% of rats dying within 14 days of treatment when administered alone. PF-318 inhibitor is an improved version of inhibitor 30 from Pfizer, which exhibited inhibitory activity toward MK2 and another related kinase MK5, with a 10-fold selectivity for MK3 (14). PF-318 has the property of 25 nM inhibitory activity toward MK2 and cellular potency of 255 nM (14). Additionally, while PF-318 was expected to exhibit reduced hepatotoxicity compared with inhibitor 30, it resulted in significant toxicity with enhanced exposure and plasma concentrations (14, 36). We made similar observations in our study when this inhibitor was administered alone to the rats without any PAN-induced damage, while reduced toxicity was observed during NS, which could have resulted from increased clearance from the plasma.

Among the major substrates of MK2 and MK3 are sHSPs. sHSPs display diverse biological functions, ranging from modulators of apoptosis to chaperones (9, 17, 55). Importantly, one of the sHSPs, HSPB1, has been reported to be antiapoptotic, and a regulator of cytoskeletal arrangement in podocytes (47, 49, 50). Moreover, most of the effects of HSPB1, such as regulation of actin filament dynamics and cell chemotaxis and exocytosis, are mediated via its phosphorylation by its upstream kinase, MK2 (11, 19, 27, 39). Furthermore, another sHSP, HSPB8, has previously been shown to form heterooligomeric complexes with HSPB1 and is also involved in the regulation of cell signaling and death (1, 54). GRP78 is another highly conserved HSP, which has been shown to play an immunoregulatory role during infection (12). In summary, sHSPs are well known to play critical roles in the cellular response to stress, and clarifying their regulation by MK2 and MK3 in NS could significantly enhance our understanding of the pathophysiology of glomerular disease and also identify novel potential future targets for therapy. Our findings clearly suggest that renal cortical HSPB1 was induced by ADR injury and that MK2 in particular plays a critical role in the phosphorylation and activation of HSPB1 in the renal cortex.

COX-2 plays an important role in kidney and podocyte physiology, and its overexpression in podocytes increases renal or podocyte susceptibility to injury (3, 7, 8, 22, 26). We recently reported p38 MAPK- and MK2-dependent induction of COX-2 expression in podocytes following exposure to serum albumin (3, 38). Moreover, mechanical stretch has been reported to induce the production of both COX-2 and prostaglandin EP4 receptor in a p38 MAPK-dependent manner in podocytes (35). Furthermore, COX-2 expression is also part of a stress response, its expression being regulated by heat shock transcription factors (45). Additionally, the p38 MAPK signaling cascade has been reported to regulate the stability of proinflammatory mRNAs such as COX-2 via its 3'-untranslated region by phosphorylated and activated MK2 and HSPB1 (33). In the present study, we have extended these findings by studying the regulation of COX-2 by MK2 and/or MK3 in ADR-induced NS. As expected, COX-2 was significantly reduced in untreated MK2^{-/-}, MK3^{-/-}, and MK2^{-/-}MK3^{-/-} groups compared with WT, which likely resulted from decreased COX-2 mRNA stability in the absence of these kinases. Furthermore, while ADR injury did not result in significant induction of COX-2 in WT mice, COX-2 was significantly induced in the renal cortex of mice lacking MK2, suggest-

ing that perhaps ADR, in the absence of MK2, directly or indirectly induced an increase in renal cortical COX-2 expression.

In summary, the current study suggests that while the inhibition of MK2 and/or MK3 regulates the renal stress response, it does not significantly reduce proteinuria in experimental models of NS and could impart toxic effects. Together, these data and our previous studies (20) suggest that our currently available approaches are not yet able to safely and effectively reduce proteinuria in experimental NS and that other p38 MAPK downstream targets (i.e., other cytosolic substrates, chromatin remodelers, and transcription factors) (10, 18) should also be considered to improve the future treatment of glomerular disease.

ACKNOWLEDGMENTS

We thank Matthias Gaestel for providing the MK2/3 knockout heterozygous pair on the C57 background. We thank Pfizer, especially Robert J. Mourey, Jean-Baptiste Teliez, and Donnie W Owens at Pfizer, for assistance in providing the MK2 inhibitor PF-318 (PF-04357318).

Present address for X. Nie: Dept. of Pediatrics, Fuzhou Dongfang Hospital, Xiamen Univ., Fuzhou, China.

GRANTS

This work was supported in part by National Institute of Diabetes and Digestive and Kidney Diseases Grant R01-DK-077283 and internal funds from Nationwide Children's Hospital (to W. E. Smoyer).

DISCLOSURES

No conflicts of interest, financial or otherwise, are declared by the authors.

AUTHOR CONTRIBUTIONS

R.P., S.A., and W.E.S. conceived and designed research; X.N., M.A.C., R.P., D.B.T., and S.A. performed experiments; X.N., M.A.C., R.P., D.B.T., S.A., and W.E.S. analyzed data; X.N., M.A.C., D.B.T., S.A., and W.E.S. interpreted results of experiments; X.N., M.A.C., D.B.T., and S.A. prepared figures; X.N., D.B.T., and S.A. drafted manuscript; S.A. and W.E.S. edited and revised manuscript; X.N., M.A.C., R.P., D.B.T., S.A., and W.E.S. approved final version of manuscript.

REFERENCES

- Acunzo J, Katsogiannou M, Rocchi P. Small heat shock proteins HSP27 (HspB1), α B-crystallin (HspB5) and HSP22 (HspB8) as regulators of cell death. *Int J Biochem Cell Biol* 44: 1622–1631, 2012. doi:10.1016/j.biocel.2012.04.002.
- Agrawal S, Chanley MA, Westbrook D, Nie X, Kitao T, Guess AJ, Benndorf R, Hidalgo G, Smoyer WE. Pioglitazone enhances the beneficial effects of glucocorticoids in experimental nephrotic syndrome. *Sci Rep* 6: 24392, 2016. doi:10.1038/srep24392.
- Agrawal S, Guess AJ, Chanley MA, Smoyer WE. Albumin-induced podocyte injury and protection are associated with regulation of COX-2. *Kidney Int* 86: 1150–1160, 2014. doi:10.1038/ki.2014.196.
- Anderson DR, Meyers MJ, Kurumbail RG, Caspers N, Poda GI, Long SA, Pierce BS, Mahoney MW, Mourey RJ. Benzothiofene inhibitors of MK2. Part 1: structure-activity relationships, assessments of selectivity and cellular potency. *Bioorg Med Chem Lett* 19: 4878–4881, 2009. doi:10.1016/j.bmcl.2009.02.015.
- Anderson DR, Meyers MJ, Kurumbail RG, Caspers N, Poda GI, Long SA, Pierce BS, Mahoney MW, Mourey RJ, Parikh MD. Benzothiofene inhibitors of MK2. Part 2: improvements in kinase selectivity and cell potency. *Bioorg Med Chem Lett* 19: 4882–4884, 2009. doi:10.1016/j.bmcl.2009.02.017.
- Chávez Valencia V, Orizaga de La Cruz C, Becerra Fuentes JG, Fuentes Ramírez F, Parra Michel R, Aragaki Y, Márquez Magaña I, Pazarín Villaseñor HL, Villanueva Pérez MA, García Cárdenas MA. [Epidemiology of glomerular disease in adults: a database review]. *Gac Med Mex* 150: 403–408, 2014.
- Cheng H, Fan X, Moeckel GW, Harris RC. Podocyte COX-2 exacerbates diabetic nephropathy by increasing podocyte (pro)renin receptor expression. *J Am Soc Nephrol* 22: 1240–1251, 2011. doi:10.1681/ASN.2010111149.
- Cheng H, Wang S, Jo YI, Hao CM, Zhang M, Fan X, Kennedy C, Breyer MD, Moeckel GW, Harris RC. Overexpression of cyclooxygenase-2 predisposes to podocyte injury. *J Am Soc Nephrol* 18: 551–559, 2007. doi:10.1681/ASN.2006090990.
- a. Corna D, Morigi M, Facchinetti D, Bertani T, Zoja C, Remuzzi G. Mycophenolate mofetil llimits renal damage and prolongs life in murine lupus autoimmune disease. *Kidney Int.* 51: 1583–1589, 1997.
- Cox D, Carver JA, Ecroyd H. Preventing α -synuclein aggregation: the role of the small heat-shock molecular chaperone proteins. *Biochim Biophys Acta* 1842: 1830–1843, 2014. doi:10.1016/j.bbadis.2014.06.024.
- Cuadrado A, Nebreda AR. Mechanisms and functions of p38 MAPK signalling. *Biochem J* 429: 403–417, 2010. doi:10.1042/BJ20100323.
- Damarla M, Hasan E, Boueiz A, Le A, Pae HH, Montouchet C, Kolb T, Simms T, Myers A, Kayyali US, Gaestel M, Peng X, Reddy SP, Damico R, Hassoun PM. Mitogen activated protein kinase activated protein kinase 2 regulates actin polymerization and vascular leak in ventilator associated lung injury. *PLoS One* 4: e4600, 2009. doi:10.1371/journal.pone.0004600.
- Das S, Mohapatra A, Sahoo PK. Expression analysis of heat shock protein genes during *Aeromonas hydrophila* infection in rohu, *Labeo rohita*, with special reference to molecular characterization of Grp78. *Cell Stress Chaperones* 20: 73–84, 2015. doi:10.1007/s12192-014-0527-2.
- Ehltling C, Ronkina N, Böhmer O, Albrecht U, Bode KA, Lang KS, Kotlyarov A, Radzioch D, Gaestel M, Häussinger D, Bode JG. Distinct functions of the mitogen-activated protein kinase-activated protein (MAPKAP) kinases MK2 and MK3: MK2 mediates lipopolysaccharide-induced signal transducers and activators of transcription 3 (STAT3) activation by preventing negative regulatory effects of MK3. *J Biol Chem* 286: 24113–24124, 2011. doi:10.1074/jbc.M111.235275.
- Fiore M, Forli S, Manetti F. Targeting mitogen-activated protein kinase-activated protein kinase 2 (MAPKAPK2, MK2): medicinal chemistry efforts to lead small molecule inhibitors to clinical trials. *J Med Chem* 59: 3609–3634, 2016. doi:10.1021/acs.jmedchem.5b01457.
- Fisk M, Gajendragadkar PR, Mäki-Petäjä KM, Wilkinson IB, Cheriyan J. Therapeutic potential of p38 MAP kinase inhibition in the management of cardiovascular disease. *Am J Cardiovasc Drugs* 14: 155–165, 2014. doi:10.1007/s40256-014-0063-6.
- Furuichi K, Wada T, Iwata Y, Sakai N, Yoshimoto K, Kobayashi Ki K, Mukaida N, Matsushima K, Yokoyama H. Administration of FR167653, a new anti-inflammatory compound, prevents renal ischaemia/reperfusion injury in mice. *Nephrol Dial Transplant* 17: 399–407, 2002. doi:10.1093/ndt/17.3.399.
- Gamell C, Susperregui AG, Bernard O, Rosa JL, Ventura F. The p38/MK2/Hsp25 pathway is required for BMP-2-induced cell migration. *PLoS One* 6: e16477, 2011. doi:10.1371/journal.pone.0016477.
- Genovese MC. Inhibition of p38: has the fat lady sung? *Arthritis Rheum* 60: 317–320, 2009. doi:10.1002/art.24264.
- Guay J, Lambert H, Gingras-Breton G, Lavoie JN, Huot J, Landry J. Regulation of actin filament dynamics by p38 map kinase-mediated phosphorylation of heat shock protein 27. *J Cell Sci* 110: 357–368, 1997.
- Guess AJ, Ayoob R, Chanley M, Manley J, Cajas MM, Agrawal S, Pengal R, Pyle AL, Becknell B, Kopp JB, Ronkina N, Gaestel M, Benndorf R, Smoyer WE. Crucial roles of the protein kinases MK2 and MK3 in a mouse model of glomerulonephritis. *PLoS One* 8: e54239, 2013. doi:10.1371/journal.pone.0054239.
- Hannigan MO, Zhan L, Ai Y, Kotlyarov A, Gaestel M, Huang CK. Abnormal migration phenotype of mitogen-activated protein kinase-activated protein kinase 2-/- neutrophils in Zigmund chambers containing formyl-methionyl-leucyl-phenylalanine gradients. *J Immunol* 167: 3953–3961, 2001. doi:10.4049/jimmunol.167.7.3953.
- Harris RC. COX-2 and the kidney. *J Cardiovasc Pharmacol* 47, Suppl 1: S37–S42, 2006. doi:10.1097/00005344-200605001-00007.
- Hegen M, Gaestel M, Nickerson-Nutter CL, Lin LL, Teliez JB. MAPKAP kinase 2-deficient mice are resistant to collagen-induced arthritis. *J Immunol* 177: 1913–1917, 2006. doi:10.4049/jimmunol.177.3.1913.
- Hogan J, Radhakrishnan J. The treatment of idiopathic focal segmental glomerulosclerosis in adults. *Adv Chronic Kidney Dis* 21: 434–441, 2014. doi:10.1053/j.ackd.2014.03.016.
- Jefferson JA, Shankland SJ. The pathogenesis of focal segmental glomerulosclerosis. *Adv Chronic Kidney Dis* 21: 408–416, 2014. doi:10.1053/j.ackd.2014.05.009.
- Jo YI, Cheng H, Wang S, Moeckel GW, Harris RC. Puromycin induces reversible proteinuric injury in transgenic mice expressing cyclooxygen-

- ase-2 in podocytes. *Nephron, Exp Nephrol* 107: e87–e94, 2007. doi:10.1159/000108653.
27. Jog NR, Jala VR, Ward RA, Rane MJ, Haribabu B, McLeish KR. Heat shock protein 27 regulates neutrophil chemotaxis and exocytosis through two independent mechanisms. *J Immunol* 178: 2421–2428, 2007. doi:10.4049/jimmunol.178.4.2421.
 28. Kang SW, Natarajan R, Shahed A, Nast CC, LaPage J, Mundel P, Kashtan C, Adler SG. Role of 12-lipoxygenase in the stimulation of p38 mitogen-activated protein kinase and collagen alpha5(IV) in experimental diabetic nephropathy and in glucose-stimulated podocytes. *J Am Soc Nephrol* 14: 3178–3187, 2003. doi:10.1097/01.ASN.0000099702.16315.DE.
 29. Kiffel J, Rahimzadeh Y, Trachtman H. Focal segmental glomerulosclerosis and chronic kidney disease in pediatric patients. *Adv Chronic Kidney Dis* 18: 332–338, 2011. doi:10.1053/j.ackd.2011.03.005.
 30. Koshikawa M, Mukoyama M, Mori K, Suganami T, Sawai K, Yoshioka T, Nagae T, Yokoi H, Kawachi H, Shimizu F, Sugawara A, Nakao K. Role of p38 mitogen-activated protein kinase activation in podocyte injury and proteinuria in experimental nephrotic syndrome. *J Am Soc Nephrol* 16: 2690–2701, 2005. doi:10.1681/ASN.2004121084.
 31. Köther K, Nordhoff C, Masemann D, Varga G, Bream JH, Gaestel M, Wixler V, Ludwig S. MAPKAP kinase 3 suppresses Ifng gene expression and attenuates NK cell cytotoxicity and Th1 CD4 T-cell development upon influenza A virus infection. *FASEB J* 28: 4235–4246, 2014. doi:10.1096/fj.14-249599.
 32. Kotlyarov A, Neininger A, Schubert C, Eckert R, Birchmeier C, Volk HD, Gaestel M. MAPKAP kinase 2 is essential for LPS-induced TNF-alpha biosynthesis. *Nat Cell Biol* 1: 94–97, 1999. doi:10.1038/10061.
 33. Lasa M, Mahtani KR, Finch A, Brewer G, Saklatvala J, Clark AR. Regulation of cyclooxygenase 2 mRNA stability by the mitogen-activated protein kinase p38 signaling cascade. *Mol Cell Biol* 20: 4265–4274, 2000. doi:10.1128/MCB.20.12.4265-4274.2000.
 34. Ma FY, Liu J, Nikolic-Paterson DJ. The role of stress-activated protein kinase signaling in renal pathophysiology. *Braz J Med Biol Res* 42: 29–37, 2009. doi:10.1590/S0100-879X2008005000049.
 35. Martineau LC, McVeigh LI, Jasmin BJ, Kennedy CR. p38 MAP kinase mediates mechanically induced COX-2 and PG EP4 receptor expression in podocytes: implications for the actin cytoskeleton. *Am J Physiol Renal Physiol* 286: F693–F701, 2004. doi:10.1152/ajprenal.00331.2003.
 36. Morris DL, O'Neil SP, Devraj RV, Portanova JP, Gilles RW, Gross CJ, Curtiss SW, Komocsar WJ, Garner DS, Happa FA, Kraus LJ, Nikula KJ, Monahan JB, Selness SR, Galluppi GR, Shevlin KM, Kramer JA, Walker JK, Messing DM, Anderson DR, Mourey RJ, Whiteley LO, Daniels JS, Yang JZ, Rowlands PC, Alden CL, Davis JW II, Sagartz JE. Acute lymphoid and gastrointestinal toxicity induced by selective p38alpha map kinase and map kinase-activated protein kinase-2 (MK2) inhibitors in the dog. *Toxicol Pathol* 38: 606–618, 2010. doi:10.1177/0192623310367807.
 37. Mourey RJ, Burnette BL, Brustkern SJ, Daniels JS, Hirsch JL, Hood WF, Meyers MJ, Mnich SJ, Pierce BS, Saabye MJ, Schindler JF, South SA, Webb EG, Zhang J, Anderson DR. A benzothiazophene inhibitor of mitogen-activated protein kinase-activated protein kinase 2 inhibits tumor necrosis factor alpha production and has oral anti-inflammatory efficacy in acute and chronic models of inflammation. *J Pharmacol Exp Ther* 333: 797–807, 2010. doi:10.1124/jpet.110.166173.
 38. Pengal R, Guess AJ, Agrawal S, Manley J, Ransom RF, Mourey RJ, Benndorf R, Smoyer WE. Inhibition of the protein kinase MK-2 protects podocytes from nephrotic syndrome-related injury. *Am J Physiol Renal Physiol* 301: F509–F519, 2011. doi:10.1152/ajprenal.00661.2010.
 39. Pichon S, Bryckaert M, Berrou E. Control of actin dynamics by p38 MAP kinase - Hsp27 distribution in the lamellipodium of smooth muscle cells. *J Cell Sci* 117: 2569–2577, 2004. doi:10.1242/jcs.011110.
 40. Pippin JW, Brinkkoetter PT, Cormack-Aboud FC, Durvasula RV, Hauser PV, Kowalewska J, Kroff RD, Logar CM, Marshall CB, Ohse T, Shankland SJ. Inducible rodent models of acquired podocyte diseases. *Am J Physiol Renal Physiol* 296: F213–F229, 2009. doi:10.1152/ajprenal.90421.2008.
 41. Ronkina N, Kotlyarov A, Dittrich-Breiholz O, Kracht M, Hitti E, Milarski K, Askew R, Marusic S, Lin LL, Gaestel M, Telliez JB. The mitogen-activated protein kinase (MAPK)-activated protein kinases MK2 and MK3 cooperate in stimulation of tumor necrosis factor biosynthesis and stabilization of p38 MAPK. *Mol Cell Biol* 27: 170–181, 2007. doi:10.1128/MCB.01456-06.
 42. Ronkina N, Kotlyarov A, Gaestel M. MK2 and MK3—a pair of isoenzymes? *Front Biosci* 13: 5511–5521, 2008. doi:10.2741/3095.
 43. Ronkina N, Menon MB, Schwermann J, Arthur JS, Legault H, Telliez JB, Kayyali US, Nebreda AR, Kotlyarov A, Gaestel M. Stress induced gene expression: a direct role for MAPKAP kinases in transcriptional activation of immediate early genes. *Nucleic Acids Res* 39: 2503–2518, 2011. doi:10.1093/nar/gkq1178.
 44. Ronkina N, Menon MB, Schwermann J, Tiedje C, Hitti E, Kotlyarov A, Gaestel M. MAPKAP kinases MK2 and MK3 in inflammation: complex regulation of TNF biosynthesis via expression and phosphorylation of tristetraproline. *Biochem Pharmacol* 80: 1915–1920, 2010. doi:10.1016/j.bcp.2010.06.021.
 45. Rossi A, Coccia M, Trotta E, Angelini M, Santoro MG. Regulation of cyclooxygenase-2 expression by heat: a novel aspect of heat shock factor 1 function in human cells. *PLoS One* 7: e31304, 2012. doi:10.1371/journal.pone.0031304.
 46. Rousseau S, Dolado I, Beardmore V, Shpiro N, Marquez R, Nebreda AR, Arthur JS, Case LM, Tessier-Lavigne M, Gaestel M, Cuenda A, Cohen P. CXCL12 and C5a trigger cell migration via a PAK1/2-p38alpha MAPK-MAPKAP-K2-HSP27 pathway. *Cell Signal* 18: 1897–1905, 2006. doi:10.1016/j.cellsig.2006.02.006.
 47. Sanchez-Niño MD, Sanz AB, Sanchez-Lopez E, Ruiz-Ortega M, Benito-Martin A, Saleem MA, Mathieson PW, Mezzano S, Egido J, Ortiz A. HSP27/HSPB1 as an adaptive podocyte antiapoptotic protein activated by high glucose and angiotensin II. *Lab Invest* 92: 32–45, 2012. doi:10.1038/labinvest.2011.138.
 48. Shiryaev A, Moens U. Mitogen-activated protein kinase p38 and MK2, MK3 and MK5: ménage à trois or ménage à quatre? *Cell Signal* 22: 1185–1192, 2010. doi:10.1016/j.cellsig.2010.03.002.
 49. Smoyer WE, Ransom R, Harris RC, Welsh MJ, Lutsch G, Benndorf R. Ischemic acute renal failure induces differential expression of small heat shock proteins. *J Am Soc Nephrol* 11: 211–221, 2000.
 50. Smoyer WE, Ransom RF. Hsp27 regulates podocyte cytoskeletal changes in an in vitro model of podocyte process retraction. *FASEB J* 16: 315–326, 2002. doi:10.1096/fj.01-0681com.
 51. Stambe C, Atkins RC, Hill PA, Nikolic-Paterson DJ. Activation and cellular localization of the p38 and JNK MAPK pathways in rat crescentic glomerulonephritis. *Kidney Int* 64: 2121–2132, 2003. doi:10.1046/j.1523-1755.2003.00324.x.
 52. Stambe C, Nikolic-Paterson DJ, Hill PA, Dowling J, Atkins RC. p38 Mitogen-activated protein kinase activation and cell localization in human glomerulonephritis: correlation with renal injury. *J Am Soc Nephrol* 15: 326–336, 2004. doi:10.1097/01.ASN.0000108520.63445.E0.
 53. Tan HY, Ng TW. Accurate step wedge calibration for densitometry of electrophoresis gels. *Opt Commun* 281: 3013–3017, 2008. doi:10.1016/j.optcom.2008.01.012.
 54. Uversky VN, Oldfield CJ, Dunker AK. Showing your ID: intrinsic disorder as an ID for recognition, regulation and cell signaling. *J Mol Recognit* 18: 343–384, 2005. doi:10.1002/jmr.747.
 55. Vertii A, Hakim C, Kotlyarov A, Gaestel M. Analysis of properties of small heat shock protein Hsp25 in MAPK-activated protein kinase 2 (MK2)-deficient cells: MK2-dependent insolubilization of Hsp25 oligomers correlates with susceptibility to stress. *J Biol Chem* 281: 26966–26975, 2006. doi:10.1074/jbc.M602134200.
 56. Wada T, Furuichi K, Sakai N, Hisada Y, Kobayashi K, Mukaida N, Tomosugi N, Matsushima K, Yokoyama H. Involvement of p38 mitogen-activated protein kinase followed by chemokine expression in crescentic glomerulonephritis. *Am J Kidney Dis* 38: 1169–1177, 2001. doi:10.1053/ajkd.2001.29206.
 57. Zakowski V, Keramas G, Kilian K, Rapp UR, Ludwig S. Mitogen-activated 3p kinase is active in the nucleus. *Exp Cell Res* 299: 101–109, 2004. doi:10.1016/j.yexcr.2004.05.027.
 58. Zaru R, Ronkina N, Gaestel M, Arthur JS, Watts C. The MAPK-activated kinase Rsk controls an acute Toll-like receptor signaling response in dendritic cells and is activated through two distinct pathways. *Nat Immunol* 8: 1227–1235, 2007. doi:10.1038/ni1517.
 59. Zheng Z, Pavlidis P, Chua S, D'Agati VD, Gharavi AG. An ancestral haplotype defines susceptibility to doxorubicin nephropathy in the laboratory mouse. *J Am Soc Nephrol* 17: 1796–1800, 2006. doi:10.1681/ASN.2005121373.
 60. Zheng Z, Schmidt-Ott KM, Chua S, Foster KA, Frankel RZ, Pavlidis P, Barasch J, D'Agati VD, Gharavi AG. A Mendelian locus on chromosome 16 determines susceptibility to doxorubicin nephropathy in the mouse. *Proc Natl Acad Sci USA* 102: 2502–2507, 2005. doi:10.1073/pnas.0409786102.